

**AN INVESTIGATION OF PRESERVATION TECHNIQUES FOR CREATING A
FULL COMPARTMENT PHANTOM**

A Thesis

by

ALICE JEAN DALE

Submitted to the Office of Graduate and Professional Studies of
Texas A&M University
in partial fulfillment of the requirements for the degree of

MASTER OF SCIENCE

Chair of Committee,	Stephen Guetersloh
Committee Members,	John Ford
	John Lawler
Head of Department,	Yassan Hassan

August 2014

Major Subject: Health Physics

Copyright 2014 Alice Jean Dale

ABSTRACT

This project is an investigation of the viability of preservation techniques for use in developing phantoms for use in Dual Energy X-ray Absorptiometry (DXA) and Computed Tomography (CT) imaging. Two rats were preserved in PEG (polyethylene glycol) or MTMS (methyltrimethoxysilane) following naval archeology preservation techniques and plastination. These subjects were imaged before and after preservation using Computed Tomography (CT) imaging and Dual X-ray Absorptiometry (DXA) body composition techniques.

The initial scanning of each of the rats used DXA and CT to provide a standard for results to compare the specimens after preservation. The rat used for MTMS preservation was larger and provided better CT imaging both before and after preservation, while the rat used for PEG impregnation was smaller and the contrast for organ identification was limited both before and after PEG preservation. However, MTMS preservation still affected the Hounsfield values and many internal organs such as the liver and brain shrank after the completion of the plastination process. The PEG preservation appeared to have homogenized HU numbers when compared to the initial scans and produced air pockets in the final CT scans of the specimen.

The tissue composition measurements from the PEG impregnation as calculated by DXA were much more accurate when compared to the original tissue composition values. The bone mineral content was fairly accurate and unchanged for both MTMS and PEG preservation procedures, but DXA greatly overestimated the lean tissue

measurements after MTMS plastination and calculated them to be much greater than the total mass. The DXA also greatly underestimated the fat content, calculating an impossible negative mass.

The MTMS plastination lasted longer than the PEG impregnation. It is possible the PEG preservation did not penetrate into the internal organs and tissues and the specimen continued to decompose in the weeks following the experiment. The MTMS preservation specimen is still well preserved three years later.

DEDICATION

This thesis is dedicated to Jimmy Uhlemeyer. Without his patience, support, and love, I never would have made it through.

ACKNOWLEDGEMENTS

I would like to thank everyone who contributed to this project and especially my Committee Chair Dr. Stephen Guetersloh for his guidance and support during this long road, as well as the rest of my Thesis Committee, Drs. John Ford and John Lawler. I would like to thank the Netum Steed Laboratory for the use of their DXA equipment and Chang Wook Lee for operating it, and the Texas A&M Institute for Preclinical Studies for the use of their CT scanner and Dr. Mark Lenox for operating it.

I would also like to thank my friends and colleagues and the faculty and staff of Department of Nuclear Engineering for the wonderful experiences and opportunities I have been given throughout my time as a student here.

I would also like to thank the University of Kansas for allowing me to continue my education, and especially Michael Lemon for his support and infinite patience.

And finally, I would like to thank my mother and father who are a never ending source of encouragement to get this done. This is for you.

NOMENCLATURE

BMC	Bone Mineral Content
CT	Computed Tomography
DXA	Dual Energy X-ray Absorptiometry
HU	Hounsfield Unit
MTMS	Methyltrimethoxysilane
PEG	Polyethylene Glycol
Ratigan	MTMS Rat Specimen
Splinter	PEG Rat Specimen

TABLE OF CONTENTS

ABSTRACT	ii
DEDICATION	iv
ACKNOWLEDGEMENTS	v
NOMENCLATURE.....	vi
TABLE OF CONTENTS	vii
LIST OF FIGURES.....	ix
LIST OF TABLES	xi
1. INTRODUCTION AND STATEMENT OF THE PROBLEM.....	1
2. LITERATURE REVIEW	4
2.1 Preservation Chemicals.....	5
2.1.1 Methyltrimethoxysilane (MTMS)	7
2.1.2 Polyethylene Glycol (PEG).....	8
2.2 Radiographic Imaging and Analysis Techniques.....	10
2.2.1 Dual Energy X-ray Absorptiometry (DXA).....	10
2.2.2 Computed Tomography.....	14
2.3 Rat Anatomy	17
3. MATERIALS AND METHODS	22
3.1 Specimen Selection	22
3.2 Radiographic Imaging.....	23
3.2.1 CT Scan Equipment and Protocols.....	23
3.2.2 DXA Scan Equipment and Protocols	24
3.3 Specimen Preservation	25
3.3.1 MTMS	26
3.3.2 PEG	26
4. RESULTS AND ANALYSIS	27
4.1 MTMS	27
4.1.1 DXA Results.....	28
4.1.2 CT Analysis.....	29
4.2 Polyethylene Glycol (PEG).....	40
4.2.1 DXA Results.....	40

4.2.2 CT Results and Analysis	41
5. CONCLUSIONS AND FUTURE WORK	48
REFERENCES	50

LIST OF FIGURES

Figure 2-1. Structural formula of MTMS.....	8
Figure 2-2. Structural formula of PEG.....	10
Figure 2-3. Comparison of Attenuation and Mass Attenuation Coefficients for Soft Tissue and Bone for use in DXA and CT.....	11
Figure 2-4. Mass attenuation coefficients for Cortical bone, Soft tissue, MTMS, and PEG.	16
Figure 2-5. Rat brain anatomy image.....	18
Figure 2-6. Rat lung anatomy image.....	18
Figure 2-7. Rat intestinal anatomy image.	19
Figure 2-8. Rat liver anatomy image.....	20
Figure 4-1. 2014 Image of Ratigan after preservation with MTMS..	28
Figure 4-2. Pre MTMS plastination total body CT image.	31
Figure 4-3. Post MTMS plastination total body CT image.....	31
Figure 4-4. Pre MTMS preservation brain and liver CT image and analysis..	32
Figure 4-5. Post MTMS preservation brain CT image and analysis.	32
Figure 4-6. Comparison CT image of brain width before and after MTMS plastination.	33
Figure 4-7. Pre MTMS plastination analysis of skin..	34
Figure 4-8. Post MTMS plastination analysis of skin and bone.	35
Figure 4-9. Pre MTMS plastination analysis of bone.	35
Figure 4-10. Post MTMS preservation liver CT image and analysis.....	36
Figure 4-11. Initial kidney distance measurements.....	37

Figure 4-12. Final kidney distance measurements.....	38
Figure 4-13. Pre MTMS preservation lung CT image and analysis.....	39
Figure 4-14. Post MTMS preservation lung CT image and analysis.....	39
Figure 4-15. Initial total body image of Splinter before PEG impregnation.....	42
Figure 4-16. Total body image after PEG impregnation of Splinter.....	43
Figure 4-17. Pre PEG impregnation brain, lungs and kidney CT image and analysis.....	44
Figure 4-18. Pre PEG impregnation brain, lungs, kidney, skin, and bone CT image and analysis.	44
Figure 4-19. Pre PEG impregnation analysis of skin.	45
Figure 4-20. Pre PEG impregnation analysis of bone.	46

LIST OF TABLES

Table 4-1. DXA measurements of pre- and post-MTMS preservation of Ratigan.....	28
Table 4-2. DXA Measurements of pre and post PEG preservation of Splinter.	40

1. INTRODUCTION AND STATEMENT OF THE PROBLEM

Not long after Roentgen discovered the x-ray, doctors have used radiographic imaging as a non-invasive way to look inside the human body. As technology has developed, so has the interest in calibrating these radiation imaging machines to get the best image for the lowest amount of radiation exposure.

A representation of the human body is used for calibration and quality assurance of radiation imaging machines. This representation is called a phantom. Many models use averaged data from the human population to develop the numbers used for a phantom and use materials that are designed to mimic the radiological properties of the sample, representing different organs in the body as “compartments.” The disadvantage with this approach is no actual sample to be imaged will be as statistically accurate as this phantom, and may necessitate additional phantoms to represent members of the population that are outliers. In addition, these tissue-equivalent materials are costly to produce and develop, leading to a very high cost of these phantoms. This often leads to multi-compartment models to only include tissue and bone, or bone, tissue, and lungs, both of which are much less than is expected to see in imaging a human torso.

The main problem with any average is that the standard deviation may be large. If the standard deviation were small, there would be little difference between any two samples, but that is often not the case with a human population. Human adult sizes range from 4 feet to 7 feet, almost twice the smaller height. Weight difference can be even more dramatic, as an athletic male can have 7% body fat while a sedentary male

may have upwards of 30, 40, or even 50%. The trend towards obesity in modern society is increasing and shows no sign of reverting to healthier levels.

Programmatic phantoms like Voxel-Man and the work of the Visible Human Project can have a large impact on the ability to create a personalized dose shaping regimen for medicinal purposes, but they cannot be used on their own. Every computer simulation must be verified by a real-life analogue, or else the user would never know if they were receiving reliable results. A reliable phantom is necessary.

There are further problems with getting a proper analogue. The perfect model would be the target subject, alive but with dosimeters stuck in key positions, in the location and stance they would be in when irradiated. For obvious reasons, this is not practical. Instead, a substitute subject is used. In order to test these plastination processes, an animal model such as a mouse or rat is an acceptable substitute, as it has been extensively studied in laboratory settings. It would be unconscionable to irradiate a living thing for no reason but diagnostics for someone else, so a dead animal is preferable. In addition living animals tend to move around if they're not restrained. This creates the need for preservation techniques for dead laboratory animals that maintain the original specimen's biological characteristics.

This project is an investigation of the viability of preservation methods and chemicals for preserving a specimen using naval archeology techniques. Many options were considered in determining which type of animal would be used as the specimen for investigating this preservation technique. The rat was selected due to its aforementioned frequent and standard use in laboratory research as well as its well-documented anatomy

and the ability to order a specimen meeting the weight requirements set by the imaging lab director in order to create a good contrast image with Computed Tomography (CT) scanners and Dual Energy X-ray Absorptiometry (DXA) devices. Large weight also means the subject will have a high body fat percentage. The imaging techniques used to evaluate these specimens were selected for their ability to image and identify different types of body tissue and their current use as investigative radiographic imaging tools.

This study is meant to illustrate the benefits and pitfalls of two chemicals and their associated methods: Polyethylene Glycol (PEG) and Methyltrimethoxysilane (MTMS). Both are meant to replace water in a dead specimen to stop the decomposition process. Bacteria and other living things that enable decomposition cannot survive in a corpse easily without water. Section 2 is the chemical composition of these preservatives, the scanning techniques used, and an overview of rat anatomy. Section 3 describes the exact materials and methods used in this study. Section 4 is a summary of the results and what they imply. Section 5 outlines what was discovered and the impact on future preservation techniques.

2. LITERATURE REVIEW

According to recent data from the Center for Disease Control (CDC), nearly 1/3 of all Americans are affected by obesity. Extreme weight gain negatively impacts nearly all systems of the human body with consequences including increased risk of coronary heart disease and high blood pressure, stroke, Type II diabetes, dyslipidemia, sleep apnea and other respiratory problems, osteoarthritis, liver and gallbladder disease, and even some cancers (endometrial, breast, colon). Because of the higher risk for health complications, it is no wonder that improving diagnostic capabilities for accurate imaging of patients with obesity is desired. (CDC 2014)

Obesity is officially defined as having a body mass index (BMI) of greater than 30. It is calculated by dividing the weight in kilograms by the height squared in meters. This number is then compared to a range of BMI values to determine weight status. Other BMI values include 18.5 as underweight, 18.5-24.9 as normal, 25.0-29.9 as overweight. However, there are many problems with using BMI as a reasonable indicator of obesity because it does not take into account fat percentage differences due to age, race, or sex. In addition, use of BMI alone may cause highly trained athletes to be diagnosed as obese due to a high BMI from increased muscle mass, not fat content. (Harp 2005, CDC 2014)

An alternative measure of obesity is looking at the fat tissue component of the body known as the body fat percentage. This is defined as the total fat mass divided by the total body mass and includes essential and non-essential body fat. (Siri 1956)

Adipose tissue provides important functions since a certain percentage of body fat is required for protection of internal organs and regulating hormone function. The recommended body fat percentage is higher for women than men due to childbearing requirements, and body fat percentage is seen as a much more reliable indicator of obesity than BMI. (Jackson et al. 2002)

There are a number of methods used to determine body fat percentage including measuring subcutaneous fat with calipers, bioelectrical impedance analysis, and the gold standard of hydrostatic weighing (Siri 1956, Jackson and Pollock 1978, Jackson et al. 1980). DXA is a new technique that has demonstrated much promise for accurately measuring bone mineral content, also has the capability to measure body composition, and is recently gaining acceptance in the medical and exercise physiology field. (Kohrt 1995, Pietrobelli et al. 2001)

Developing a technique that has the capability to economically preserve specimens in a range of sizes and shapes will allow for the study of a variety of phantoms displaying normal and pathological anatomy.

2.1 PRESERVATION CHEMICALS

Plastination refers to a process used for preserving biological specimens including whole bodies or parts. This technique was first developed by Gunther von Hagen and works by replacing the water and fat content with plastic materials. The resultant specimens do not decay and can be used for their original intended purpose for longer periods of time. Ideal plastination techniques do not sacrifice the structure or functionality of the original tissues in the specimen and can therefore be used as a long

term instructional tool. Improving on a plastination technique means maintaining the maximum number of properties of the original sample.

Standard plastination processes follow four steps. The first stage of plastination is fixation. The sample is set in the position desired for the final product. If this stage is expected to take a long time or if extra support structures are needed, a preservation material may be added to the specimen at this stage. Water is then removed from tissues using acetone during the next stage: dehydration. This is accomplished by the freezing temperatures that this step utilizes which allows the acetone to replace the water that is drawn out of the cells. The specimen is then placed in a bath of plastic solvent such as a silicone or epoxy, and the acetone is removed from the cells by vaporization in a vacuum. Performing this step in a vacuum is called “forced impregnation”. The vaporization process draws in the plastic solvent into the cells where the fat and water was originally. The speed of impregnation depends on many factors including the density and thickness of the specimen as well as the viscosity of the plastic solution. Increasing each of these factors will slow the impregnation process. The final stage is curation where the plastic material may be exposed to heat or UV light to be hardened (Hagens 1986).

Another application of chemical preservation is preserving naval archeology artifacts. These artifacts are initially waterlogged and preserved in the aquatic environment and once the artifacts have been salvaged, a conservation technology must be applied. The Archeological Research Laboratory has been researching techniques for preserving these artifacts. These artifacts are comprised of a number of materials

including wood, rope, leather, and animal tissues. PEG or polyethylene glycol has been traditionally used to preserve these artifacts because of its potential for reversibility.

The common materials for plastination promoted by Gunther von Hagens are proprietary chemicals using silicone rubber, epoxy resin, or polyester resin as base depending on the purpose or specimen type to be plastinated. (Hagens 1987) Naval archeological preservation techniques traditionally use PEG impregnation and other preservation techniques using silicone and MTMS (methyltrimethoxysilane) (Smith 1997, Smith and Hamilton 1998). This investigation uses these archeological preservation chemicals that more closely mimic biological tissue and are expected to preserve the specimens radiological properties.

2.1.1 Methyltrimethoxysilane (MTMS)

MTMS, also known as Trimethoxy(methyl)silane, reacts with water and dehydrates biological tissue releasing methanol as a byproduct. This process preserves the biological tissue allowing the subject to be studied for an extended amount of time. MTMS mimics water density closely, with a specific density of 0.955 making it a good candidate for tissue preservation (Sigma-Aldrich 2012). The chemical formula is $\text{CH}_3\text{Si}(\text{OCH}_3)_3$. When MTMS reacts with water, it strips away a hydrogen atom from a water molecule and methanol gas is released. This reaction incorporates a silicon atom into the tissue and is expected to change the density of the tissue.

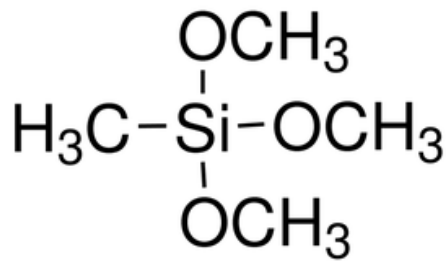


Figure 2-1. Structural formula of MTMS. (Sigma-Aldrich 2012)

After the specimen has been plasticized, the specimen becomes rigid and inflexible. Muscle and soft tissues become hard and no longer solely rely on the skeletal system for their structure. Specimens must be plasticized in the position required for the imaging techniques because they cannot be adjusted once the process is completed.

(König et al. 2013)

2.1.2 Polyethylene Glycol (PEG)

PEG can refer to a wide range of chemicals that are produced by polymerizing ethylene glycol. It will be appended by a number, such as PEG 400 or PEG 3000, referring to the average molecular weight of each polymer chain (ScienceLab.com 2005). It has a variety of applications in a number of areas including medicine and industry. In combination with acetone, it has been used with some success in preserving naval artifacts and helps prevent warping or shrinking as the artifacts dry out. It acts as a stabilizer in wooden objects by replacing water that was taken out by the acetone bath. PEG has also been used to preserve waterlogged leather artifacts by first soaking the material in acetone for 3 days to dehydrate the leather and then adding PEG to impregnate the leather. Specimens impregnated with PEG retain the pliability and

flexibility of soft tissues and joints and rely on the skeletal system of the specimen to retain its shape. After impregnation the specimen may be moved and adjusted for better imaging. (König et al. 2013)

Acetone is used to help the PEG impregnate the biological tissue by increasing the permeability of the cell membranes displacing the water in the tissues and allowing the PEG to penetrate. The PEG then reacts with the acetone in the tissue rebulking the specimen. Acetone is miscible in water and is commonly used as a solvent in organic chemistry to help mix polar and non-polar reactants. It is a ketone that is present naturally in humans and animals. (Casazza et al. 1984) It has a very low melting point, ($<-95^{\circ}\text{C}$) and can therefore be used in experiments at low temperatures. It is very volatile with a very low boiling point and high vapor pressure causing a low flash point (1°F) and making it a combustion hazard. The chemical formula for acetone is $(\text{CH}_3)_2\text{CO}$.

PEG 200 refers to its molecular weight of 200 g/mol and has a specific gravity of 1.124 making it an appropriate investigation candidate for tissue preservation. The specific gravity is slightly higher than water, which may impact the final weight of the specimen. Along with acetone, PEG has a very low melting point (-85°F) which allows for the impregnation to occur in freezing temperatures. The chemical formula is $\text{H}(\text{OCH}_2\text{CH}_2)_n\text{OH}$ and the structural formula is depicted in Figure 2-2.

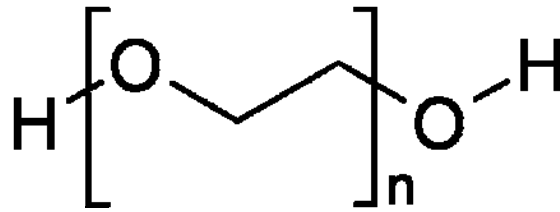


Figure 2-2. Structural formula of PEG. (ScienceLab.com 2005)

2.2 RADIOGRAPHIC IMAGING AND ANALYSIS TECHNIQUES

Two radiographic imaging techniques were used to analyze preservation techniques: Dual Energy X-ray Absorptiometry (DXA) and Computed Tomography (CT). The benefit of using each of these imaging modalities is that DXA allows for a qualitative analysis of the change in body composition, and CT allows identification of gross changes to anatomy and structure of the specimen after each preservation procedure.

2.2.1 Dual Energy X-ray Absorptiometry (DXA)

DXA, also known as “dual x-ray absorptiometry,” works by having photons of a lower and a higher energy (generally 40 keV and 70 keV, respectively) passing through the same medium and comparing the changes in the intensity of the photon beam. The DXA apparatus used in this experiment utilizes an initial x-ray energy of 70 keV and is filtered using a cerium filter that contains a k-edge of 40 keV, providing the two energy peaks necessary for DXA calculations (GEHealthcare 2012). The mass attenuation coefficient for the tissues is constant, allowing for the calculation of the mass of the tissue (Genton et al. 2002). These energies interact with the same tissues differently and

can be used to identify different types of body composition, with a particular application in the area of bone mineral density measurement (Tothill et al. 1999, Lochmüller et al. 2001). Please see Figure 2-3 for a comparison of mass attenuation coefficients for soft tissue and bone at DXA and CT energies.

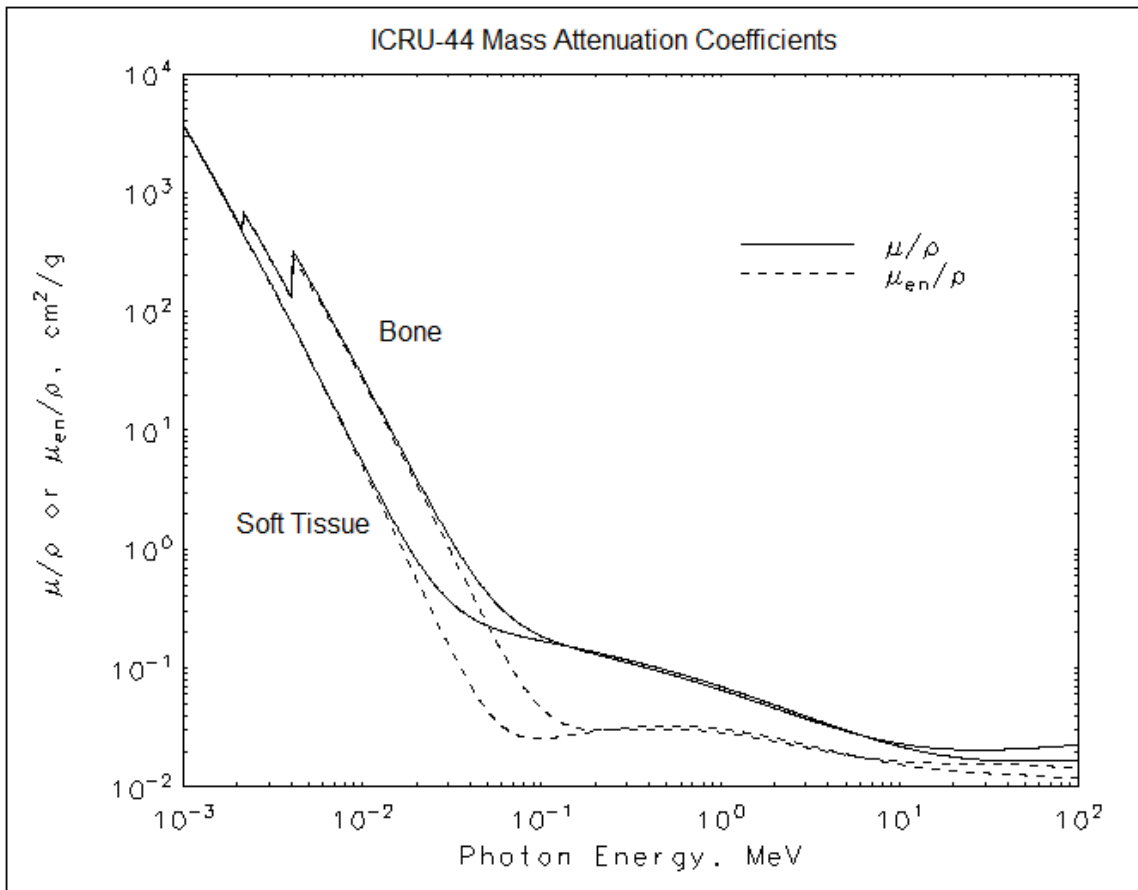


Figure 2-3. Comparison of Attenuation and Mass Attenuation Coefficients for Soft Tissue and Bone for use in DXA and CT. Adapted from ICRU-44.(ICRU 1989)

The contribution of the body mass that is comprised of bone mineral content (BMC) is separated out from soft tissue. The remaining mass is then further divided into

fat mass and lean soft tissue (fat-free) mass. By comparing the two different systems, the results are combined into total body composition analysis.

The difference in intensity in areas containing only soft tissue or soft tissue and bone is measured for both DXA x-ray energies. Likewise, the change in intensity is independently measured for both DXA x-ray energies in areas containing bone and soft tissue. The ratio of the known mass attenuation coefficients for the low to the high energy are calculated into the R-value for fat (R_F), lean tissue (R_{LM}) and BMC (R_B). The mass attenuation ratio for soft tissue is experimentally determined by DXA results for each subject and varies linearly with the amount of fat in a subject. The general relationship is described in Equation 1. (Pietrobelli et al. 2001)

$$R = \frac{\sum \mu_{i,L} x_i}{\sum \mu_{i,H} x_i} = \frac{-\ln\left(\frac{I^L}{I_0^L}\right)}{-\ln\left(\frac{I^H}{I_0^H}\right)} \quad (1)$$

Where R is the R-value, I_0 is the intensity of the radiation at the source, and I is the intensity of radiation after it has passed through tissue. A superscript of H denotes that the higher energy is used and a superscript of L denotes the lower energy. The linear attenuation factor, μx , where μ is the linear attenuation coefficient and x is thickness, is computed for each of i tissue types. Since x will be the same for both numerator and denominator, and all other factors are either known experimentally (μ) or discovered by the DXA machine (intensities), this becomes a single formula with i unknown values. It is solvable for $i \leq 2$.

It is practical to simplify the math for the computer and have R-values pre-computed in a table. This way, the computer gets the R-value from the ratio of intensities and then easily looks up what the x values should be for that R-value.

The percent of lean tissue (L) is then calculated using Equation 2.

$$\%LM = 100 \times \left(\frac{R_{ST} - R_F}{R_L - R_F} \right) \quad (2)$$

Because lean tissue is all of the tissue minus the fat content (F), the rest of the soft tissue component (ST) is considered to lean. Therefore the percentage of fat tissue can be calculated by subtracting the lean tissue percentage from 100.

So far, there have been two unknowns: amount of fat and amount of lean tissue. The two measurements taken at high and low energies are adequate to determine them. When the scanner passes over bone, however, a third unknown is encountered. Transmission through bone is significantly different from soft tissue, so it is a simple matter for the machine to determine when it is or is not over bone. Over a pixel containing bone, the scanner will assume that the composition of non-bone tissue is the same as nearby pixels, reducing the equations again to two unknowns: bone and tissue. BMC can then be calculated by taking the mass of bone found through the attenuation of the beams and dividing it by the approximate volume of the bone.

Because DXA is sensitive enough to identify the percentage of the lean muscle mass, fat, and bone density percentages, this data can be used for body composition analysis in obesity studies (Slosman et al. 1992). These measurements used to be made by hydrostatic weighing or caliper measurements, but DXA is now an accepted standard as well. Though DXA is less accurate than some destructive analyses like dry ash

sampling, it is still precise (Rose et al. 1998). The benefit of using DXA to evaluate the viability of these preservation techniques is that it can evaluate deviation of the mass of these individual types of tissues from the original natural state.

2.2.2 Computed Tomography

A CT machine uses the difference in linear attenuation coefficients of different body tissues to create images of the anatomy and produces these images as two-dimensional slices to create a 3-D model of the animal or human body. A photon beam and a detector work in tandem and rotate around a subject. An image is then reconstructed from the change in intensity of the beam and the linear attenuation coefficient is converted into a Hounsfield unit (HU). Please see Figure 2-4 for data of linear attenuation for biological tissues and preservation chemicals used in this experiment.

Hounsfield Units are the standard for CT scanners that are calibrated to water phantoms. They measure the relative difference in linear attenuation between an object and the equivalent volume of water. Since it is computed on a voxel basis, thickness of the subject is irrelevant (Seco and Evans 2006).

Attenuation at the energies of interest for CT scanners is largely dependent on Compton scattering. This is more directly a measurement of electron density than mass density. As such, introducing a medium that includes more hydrogen than an equivalent mass of water could lower the measurement in Hounsfield Units. The difference is more pronounced with bone, which contains little to no hydrogen. Since the CT scanner does not know the exact material being investigated, it cannot determine density directly. The

scale defines water as 0 HU, air as -1000 HU and bone reaching as high as 3000 HU.

The HU values are energy dependent, but air and water HU values are same at any x-ray energy (Herman 2009).

$$HU = 1000 * \frac{(\mu_x - \mu_{H_2O})}{\mu_{H_2O}} \quad (3)$$

The Texas A&M Institute for Preclinical Studies (TIPS) has provided the use of a 128-slice CT machine to observe the anatomical structure of each of the two rats before and after they have been preserved. A user can step through the image at each slice, generating a truly 3-D model of the interior of the specimen. This is useful for determining volume or conformation of organs. Information from these scans can be used to reconstruct a computer-generated model that could be utilized for phantoms. It is common in medical practices to introduce a contrast agent to further sharpen the image of specific organs or structures without the use of additional radiation.

The dose from a CT scan is much higher than DXA. According to the American Nuclear Society, a patient in a whole body scan can receive 1000 mrem, meaning a dose of 10 mGy per scan. This is because a CT scan uses higher energies, more beam intensity and exposure time, all of which contribute to the increase in the dose to the subject.

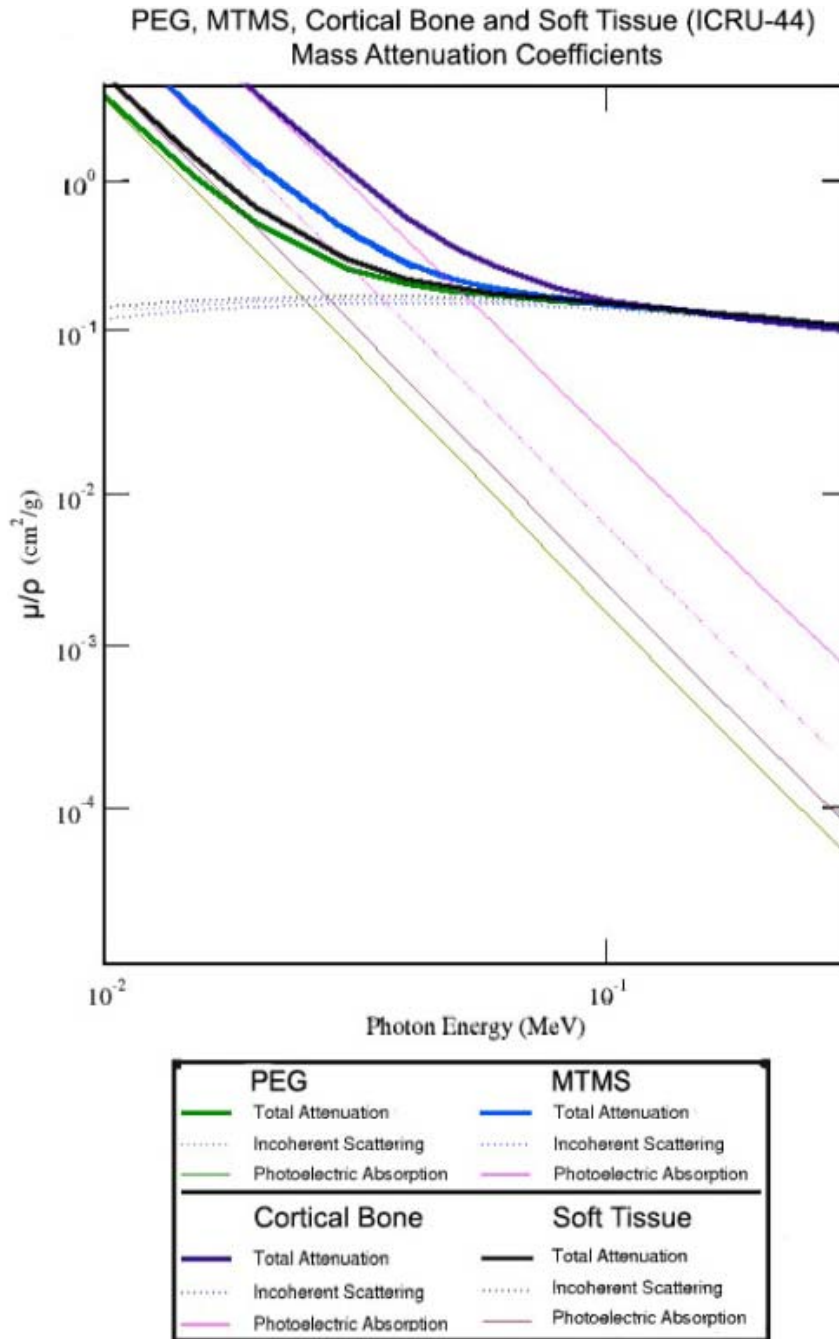


Figure 2-4. Mass attenuation coefficients for Cortical bone, Soft tissue, MTMS, and PEG. Data generated from NIST and includes total attenuation, and contributions from photoelectric and incoherent scattering for each material of interest. (Berger and Hubbell 2009)

2.3 RAT ANATOMY

The anatomy of a rat has been well characterized in previous research and was therefore chosen as the biological specimen for investigation of these preservation techniques. There are a few major anatomical differences in the internal organs when compared to humans such as a lack of tonsils and gall bladder, as well as inclusion of other glands not found in humans. However, much of the anatomy of the rat is of interest because it is similar to humans and can be easily identified by radiographic imaging such as the CT machine used in this investigation (Starks and Cutter 1931).

The brain of the rat is similar to the human brain in composition. It contains a left and a right cerebral hemisphere, as well as a cerebellum and medulla oblongata attached to top of the spinal cord, all of which are a part of the anatomy of the human brain. These regions of the brain are identified in Figure 2-5. The brain to body size ratio is 10 times larger in humans and is more elongated in shape for rats (Serendip 1994).

The lungs are an organ of interest and are unique as the left lung has only one lobe, but the right contains four. These lobes of the lung and surrounding tissues and organs are identified below in Figure 2-6. Humans have only one lobe in each lung. The anatomy of the heart is more similar to humans as it is a four chamber heart and is functionally similar (Hasenfuss 1998). Two kidneys are also identified in a rat specimen and are located more anterior in the body when compared to a human. (Greene 1935, Silverthorn 2007)

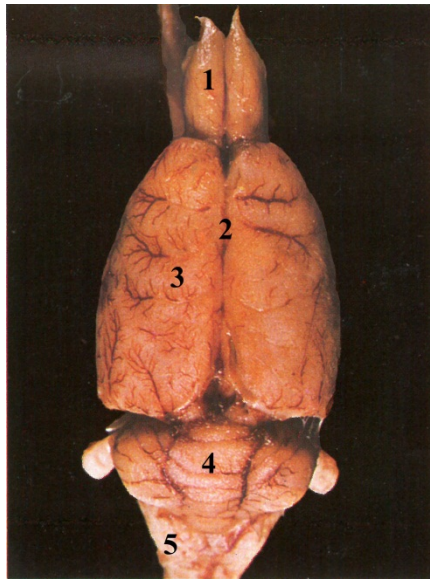


Figure 2-5. Rat brain anatomy image. Top view of the anatomy of a rat brain with important features labeled as follows: Olfactory lobe (1), Median fissure (2), Cerebral hemisphere (3), Cerebellum (4), Medulla oblongata (5). Figure adapted from Olds. (Olds and Olds 1979)

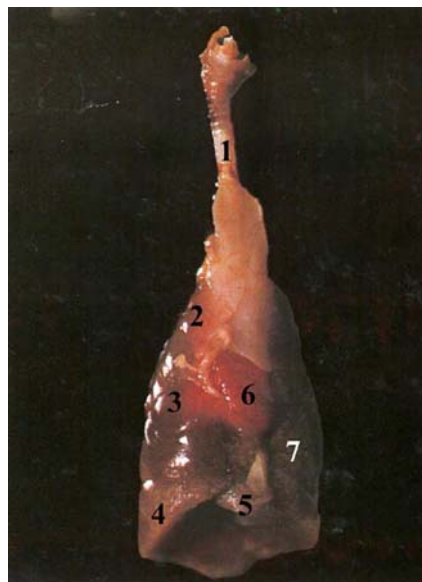


Figure 2-6. Rat lung anatomy image. The anatomy of the lung with important features identified as follows: Trachea (1); Lobes of the right lung (2-5) anterior, median, posterior, and post-caval, respectively; Heart (6), and Left lung (7). Figure adapted from Olds. (Olds and Olds 1979)

In the digestive tract labeled below in Figure 2-7, the first organ of interest is the stomach, close to which the liver can be identified. A rat liver contains 4 lobes: a large left lobe, median lobe, right lobe, and the small caudate lobe situated around the esophagus. See Figure 2-8 for identification of the liver anatomy and surrounding organs. A human liver contains 2 lobes, a left and right lobe, and is protected by the rib cage. In a rat, the small intestine is connected to the colon at the caecum, and the caecum not found in humans. It can be identified visually as a curved pouch, the large relative size of which is specific to rodents. The rest of the colon can be divided up in a similar way to the human colon, including ascending, transcending, and descending colon divisions. (Olds and Olds 1979)



Figure 2-7. Rat intestinal anatomy image. The intestinal anatomy of a rat with important organs identified as follows: Liver (1), Stomach (2), Small intestine (3), Caecum (4), Colon (5). Figure adapted from Olds. (Olds and Olds 1979)

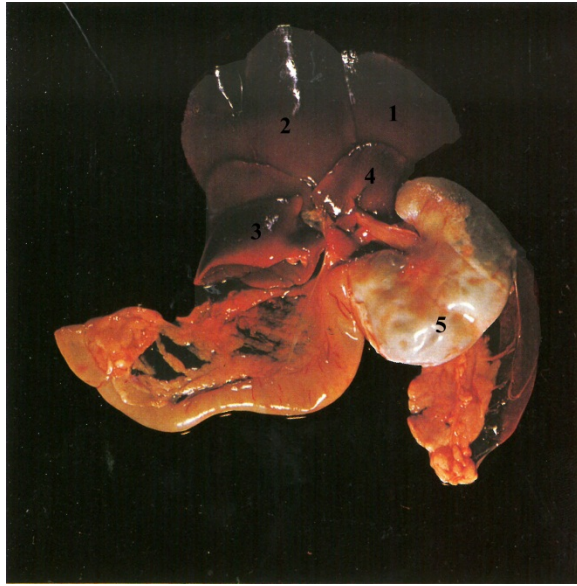


Figure 2-8. Rat liver anatomy image. A photograph of a rat liver and important features nearby organs identified as follows: Left lobe (1), Median lobe (2), Right lobe (3), Caudate lobe (4), Stomach (5). Adapted from Olds. (Olds and Olds 1979)

Skeletal imaging has always been an easy favorite for radiographers. It is readily visible on radiographs due to the large density difference between the calcium-rich bone and every other part of the body. The skeleton of the rat is similar to the skeleton of the human, possessing many bones with commensurate purposes. There are 206 bones in the adult human skeleton and 223 in the rat. The difference is mostly due to the rat's tail (Greene 1935). Anatomically, there are some other differences. Mainly, rats' epiphyses do not always fuse, allowing for longitudinal growth at much later comparative ages to humans. They do not employ Haversian remodeling like primates, but are still similar enough for studies on osteoporosis (Lelovas et al. 2008).

Other identifiable differences can be seen in the skin. Observationally, rats have much thicker fur, and it grows in patches versus a mosaic pattern for humans.

Structurally the skin is similar; both humans and rats have a dermal and epidermal layer, and thermoregulate in the same way. The integumentary system is not as tightly attached to the underlying tissues in rats as it is in humans and is also more elastic. (Starks and Cutter 1931)

3. MATERIALS AND METHODS

The project will be investigated in two parts: two different preservation chemicals will be used for plasticization of the rats. They will be compared using the before and after images from the two different radiographic imaging techniques described above: DXA and CT.

The phantoms were prepared by using an organic specimen using preservation techniques developed in the Nautical Archaeology Preservation Laboratory at Texas A&M University and based on prior plastination research. The specimen species selection and preservation process followed is discussed below. The process is to take a whole organism and preserve it by dehydrating the tissues and uploading polymers into the cellular matrix.

3.1 SPECIMEN SELECTION

Two rats were chosen as the specimens to investigate the viability of these preservation techniques due to their well-studied anatomy and common use in research protocols (Greene 1935). Because these animals are smaller than the human subjects most often imaged by the CT machine, the largest size available (greater than 500 grams) were obtained as the appropriate option to maximize the contrast of the radiographic image and provide a higher probability of useful imaging results. Rats were procured from a company that produces deceased frozen animals for the purpose of feeding reptiles to satisfy Institutional Animal Care and Use Committee (IACUC) requirements. No animals were specifically killed for the purpose of this study.

The rat specimen with a higher mass was chosen to investigate the MTMS plastination procedure because it was predicted that it would have the least change in the anatomic structure and would have a better chance of a higher resolution of images during the CT scans. This rat was named “Ratigan” for identification purposes throughout this study. The other rat was named “Splinter” and was used to investigate the PEG impregnation procedure.

3.2 RADIOGRAPHIC IMAGING

The specimens were kept frozen and placed in plastic bags for sanitary reasons before the initial imaging procedures described in Sections 3.2.1 and 3.2.2 were performed. After the completion of the radiographic imaging, the respective preservation processes described in Section 3.3 were performed. After preservation, the plastic bags were no longer necessary and were discarded.

3.2.1 CT Scan Equipment and Protocols

The 128-slice CT located at the Texas A&M Institute for Preclinical Studies (TIPS) is a Siemens Biograph PET/CT primarily used for larger specimens. A large current was therefore used (292 mAs) to increase the resolution and contrast. The CT protocol used an energy setting of 80 keV and an initial pitch of 1.4 mm and final pitch of 1.5 mm. Each slice was 0.6 mm thick and had a 1.0 second rotation time for 20 slices.

The images were analyzed using DICOM data processing software using a two dimensional (2D) analysis that measures the distance of a particular organ of interest and measures the average HU value and the range of HU values of the tissue of interest. Further analysis was performed using a three dimensional (3D) analysis volumetric

measurement that can identify the organ of interest by using a threshold minimum and maximum value to isolate the HU range of the organ tissue. These threshold values were visually set based on the best border definition and isolation of the tissue of interest. The volume, HU values, and distance were then calculated by the software for both the initial and post preservation scans and compared.

Because of the small size of the animals in the study, the CT was unable to image every organ distinctly, and the subsequent preservation procedure made certain organs unidentifiable. Therefore, the organs of interest for Ratigan and identified by the CT were limited to HU measurements of the skin, bone, brain, lung, and liver; volume measurements of the liver, lungs, and brain; and distance measurements of the brain width and kidney length. The original weight of Splinter was less than Ratigan and after preservation even less, so the ability to identify the organs of interest was reduced further. Therefore organs of interest for Splinter were then limited to HU measurements of skin, lungs, kidney, brain, and bone; and volume measurements of brain, and kidneys.

The initial scans were performed in the afternoon of November 16, 2011, two weeks prior to the start of the plastination process. The specimens were allowed to rest after the completion of both preservation processes to encourage further curating before the final CT scans were performed on January 30, 2012.

3.2.2 DXA Scan Equipment and Protocols

The DXA machine used for the qualitative analysis of the tissue content was a GE Lunar Prodigy Advance provided by the Netum Steed Laboratory. This DXA model produces the two energies of x-rays using a cerium filter that produces both x-ray

energies (40 keV and 70 keV) simultaneously. A small animal scan protocol provided by the operating software of the machine was used to measure the change in tissue content before and after the specimen's respective plastination process. Here the animals were weighed before performing the DXA scan to ensure the most accurate total mass used to calculate individual tissue content and masses. The DXA calculated the masses of the BMC, fat, and lean muscle mass of both of the specimens before and after their respective preservation procedures. These three mass determinations along with the total mass were used to calculate the percent composition of each of the three components and the difference in the percent composition from each preservation procedure was compared.

The initial scans were performed in the afternoon of November 23, 2011, 1 week prior to the start of the plastination process. The specimens were allowed to rest after the completion of both preservation processes to encourage further curation before the final DXA scans were performed on January 30, 2012.

3.3 SPECIMEN PRESERVATION

The specimens were shipped frozen and kept frozen until after the initial scans were performed and until the start of the plastination portion of the project. The specimens were washed with soap and water to remove all debris and patted dry. They were allowed to finish drying and defrosting in the refrigerator for two days after the initial DXA and CT scans were performed.

3.3.1 MTMS

The specimen identified as RATIGAN was placed in a stainless steel tray and a solution of MTMS was poured over the specimen. One liter of Sigma-Aldrich MTMS, assay grade 95 percent, (product No. 440175) was used for this procedure.

The MTMS solution was allowed to diffuse through the tissue at room temperature in a hood for 48 hours. After 48 hours, RATIGAN was removed from the tray and cleaned by rinsing the residual MTMS. The specimen was then allowed to rest at room temperature and the plasticization process was completed as the sample rested over the next three days. No catalyst was used in this process.

3.3.2 PEG

The PEG used in this investigation was PEG 200 produced by Sigma-Aldrich (product No. P3015). The advantage in using this product is its low molecular weight and closeness to human tissue density. Laboratory grade acetone was used for the dehydration stage.

The specimen designated as SPLINTER was placed in a stainless steel tray and submerged in a bath of acetone. The tray was placed into a freezer and allowed to dehydrate at -20 C for 1 week. Then acetone was replaced with a mix of 50/50 acetone and PEG and replaced in the freezer for 48 hrs. The solution was then removed and replaced with 100% PEG and rebulked into the tissue for 48 hrs under the freezing conditions. The specimen was allowed to come to room temperature and left in a hood for three days to finish off-gassing the rest of the PEG and acetone and finish the curating process. No catalyst was used in this process.

4. RESULTS AND ANALYSIS

The results were collected in the manner described in the procedure section. Visual and physical observations were taken before and after the MTMS and PEG procedures. Validation measurements of the change from the initial and post preservation state were taken at the same date and time for both preservation procedures and both used the DXA and CT protocols and equipment.

4.1 MTMS

As expected, Ratigan, the rat preserved in MTMS was hard to the touch and firmly set in position following the completion of the plastination process. The skin color tone became much darker and developed a bluish hue. After the plastination process, the total mass of Ratigan decreased from an initial weight of 0.609 kg to 0.578 kg, for a loss of 5.1%.

The MTMS preservation process has proven very effective for preserving a long term biological specimen. Today the specimen is able to be handled and the hair and whiskers are still attached. This specimen is still in the same condition as it was in the days following the MTMS preservation procedure in December 2011. Please see Figure 4-1 for a present day image of Ratigan after three years.



Figure 4-1. 2014 Image of Ratigan after preservation with MTMS. Please note the bluish color of the skin tone and preserved whiskers and fur.

4.1.1 DXA Results

Measurements of the tissue composition of Ratigan were taken using the DXA scanner. The scans were performed before and after the MTMS preservation procedure and the results found in the tissue composition are reported in Table 4-1.

Table 4-1. DXA measurements of pre- and post-MTMS preservation of Ratigan. The tissue compartment masses for bone mineral content (BMC), fat, and lean tissues are included and calculated using the total mass and DXA measurements. Specimen was scanned twice after preservation for further validation of tissue compartment values.

	Total Mass (kg)	BMC (g)	Fat (g)	Lean Tissue(g)
Initial	0.609	21.3	57	531
Final ₁	0.578	26.9	-474	1025
Final ₂	0.578	27.1	-459	1009

The tissue composition percentage was calculated using the average of the two DXA tissue mass measurements. The change in the tissue composition percentage of the BMC was an increase of 5.7 percent and resulted in the least change when compared to lean tissue and fat tissue.

The lean tissue was significantly overestimated in the post preservation and calculated to be almost twice the original lean tissue mass and significantly greater than the total mass. The difference in the tissue composition percentage of lean tissue is a very large increase of 88.8 percent. The fat tissue mass was greatly underestimated. A negative mass was calculated, resulting in a decrease of 90.1 percent in the tissue composition percentage. The reported 90 percent decrease between the initial and final fat tissue composition measurements is due to the DXA scanner's miscalculation of the mass density of the tissue in question. This shows the MTMS preservation method drastically alters the radiological properties of the tissue likely in the form of the mass attenuation coefficient. This is likely from the incorporation of silicon from the MTMS chemical structure into the tissue; however, this cannot be definitely concluded from the current study.

4.1.2 CT Analysis

Total body images and images of important organs before and after the MTMS preservation procedure were obtained and described here. Measurements of the change in the HU values, size, and shape of these organs from before and after the preservation were made using the CT imaging processing software. Ratigan was larger than the PEG rat (Splinter) and more detail in the organs was able to be imaged. The MTMS

preservation process shrunk several organs in size and increased the HU values of some of the tissues, and therefore more details were able to be imaged and identified before the preservation process. The measurements described below include volumetric analysis of the brain, liver, and lungs; linear distance measurements of the lungs, brain, and kidneys; and changes to the HU values for the brain, skin, bone, liver, and lungs. Total body CT images are presented in Figure 4-2 and Figure 4-3.

The brain is an important organ of interest that demonstrated a notable change in size after plastination. The volume decreased significantly and was measured using a 3 dimensional volumetric measurement described above. The initial volume was 1.08 cm^3 but it decreased to 0.42 cm^3 after the MTMS process for a change of 61.1 percent. This decrease is likely due to the MTMS not penetrating into the tissue, and not maintaining the structure of the organ during the dehydration of the tissue. The initial volumetric measurement of the brain can be identified on Figure 4-4, and the final volumetric analysis of the brain can be identified in Figure 4-5.

The change in width of the brain is also significant and further displays the shrinkage of the brain from the dehydration and preservation process. Visual inspection of the slices was used to determine the widest section of the brain and the software was used to measure this distance. The initial width was 1.45 cm and after preservation shrank to 1.34 cm, resulting in a decrease of 7.59 percent. The smaller diameter of the brain can be clearly seen in the comparison of the initial and final slice of the brain located in Figure 4-6.



Figure 4-2. Pre MTMS plastination total body CT image. This is a longitudinal slice of the bottom view of Ratigan.



Figure 4-3. Post MTMS plastination total body CT image. This is a longitudinal slice of the top view of Ratigan.



Figure 4-4. Pre MTMS preservation brain and liver CT image and analysis. Volumetric, maximum distance, and HU measurements of the brain (2) and liver (3) of Ratigan were analyzed using 3-D modeling image processing.



Figure 4-5. Post MTMS preservation brain CT image and analysis. Volumetric and HU measurements of the brain of Ratigan were analyzed using 3-D modeling image processing.

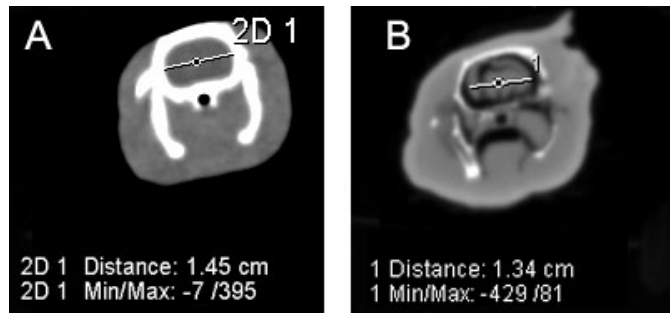


Figure 4-6. Comparison CT image of brain width before and after MTMS plastination. Width measurements of the brain before (A) and after (B) MTMS preservation of Ratigan were taken using 2D image processing software using the visually identified slice with the greatest width.

The HU measurement in the brain was also altered after preservation. The initial HU values of the brain as reported in Figure 4-4 are maximum value of 21 HU to a minimum value of -20 HU, averaging 4 HU. The HU values in the brain after preservation with MTMS range from -100 to 100 HU with an average of 7 HU, and are reported in Figure 4-5.

The HU value of the skin tissue was increased significantly. The initial HU values of the skin are reported in Figure 4-7 and range from -40 to 23 HU with an average of 6.3 ± 19 HU. The final HU values after Ratigan was preserved with MTMS are reported in Figure 4-8 and range from -190 to 424 HU and average 309.6 ± 161.4 HU. In the final total body image located in Figure 4-3 and the cross-section image in Figure 4-8, the skin appears thicker when compared to the initial images located in Figure 4-2 and Figure 4-7. This may be from a layer of MTMS forming subdermally, suggesting either MTMS passed slower into the organs than skin, or that skin still allowed MTMS to pass through after the tissues were saturated.

The bone HU measurements also appeared to increase from an initial range of 101 to 952 HU as depicted in with an average of 631.1 ± 208.6 HU as reported in Figure 4-9 to a range of 1241 to 1568 HU with an average of 1432.6 ± 86.2 after preservation in MTMS. The final HU measurements are, together with skin HU values, in Figure 4-8.



Figure 4-7. Pre MTMS plastination analysis of skin. Initial skin average and range of HU values for Ratigan were measured using 2D image processing software.

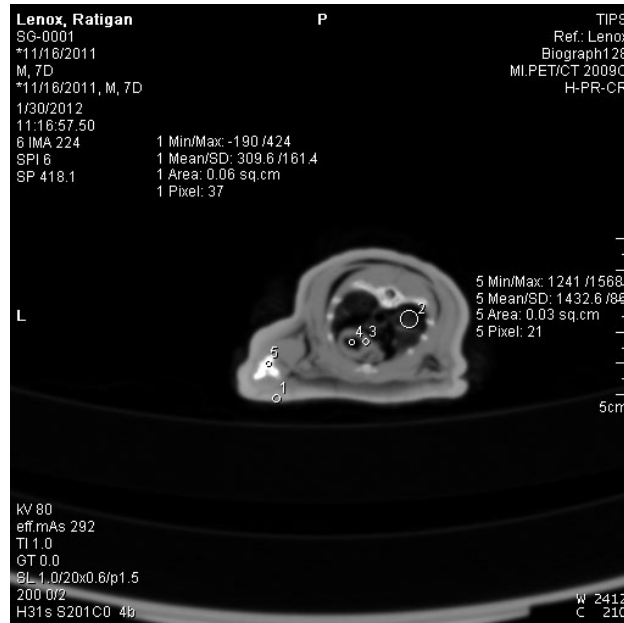


Figure 4-8. Post MTMS plastination analysis of skin and bone. Final HU analysis of skin (1) and bone (5) average and range of HU values for Ratigan were measured using 2D image processing software.

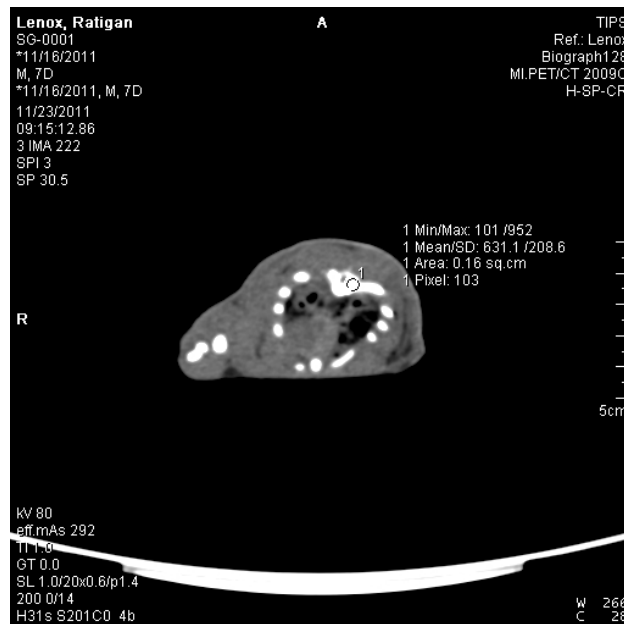


Figure 4-9. Pre MTMS plastination analysis of bone. Initial bone average and range of HU values for Ratigan were measured using 2D image processing software.

The volumetric measurements of the liver were calculated before and after MTMS preservation using the 3D model previously described. The initial volume of the liver is reported in Fig. 4-3 and was calculated to be 10.44 cm³. The liver after the MTMS preservation shrank significantly to 1.23 cm³. This decrease is likely due to the MTMS not penetrating into the tissue, and not maintaining the structure of the organ during the dehydration and preservation of the tissue.



Figure 4-10. Post MTMS preservation liver CT image and analysis. Volumetric and HU measurements of the brain of Ratigan were analyzed using 3-D modeling image processing.

The initial range of the liver tissue was -30 to 109 HU with an average of 13 HU. The HU measurements did not appear to change greatly after preservation and ranges from -101 to 124 HU with an average value of 14 HU.



Figure 4-11. Initial kidney distance measurements. Measurements of the length of the kidney before MTMS plastination were taken using 2D image processing software.

The longitudinal measurement of the kidney was taken before and after MTMS preservation. The initial distance was 1.95 cm and after preservation was found to be 1.93 cm. This is a decrease of 1.0 percent and did not appear to radically alter the structure and size of the organ during the dehydration and MTMS preservation procedure. See Figure 4-11 for initial measurement and Figure 4-12 for the final measurement.



Figure 4-12. Final kidney distance measurements. Measurements of the length of the kidney after MTMS plastination were taken using 2D image processing software.

The initial HU values of Ratigan in the lungs range from -102 to 50 HU and average -17 HU. After MTMS preservation, the HU values in the lungs decreased significantly to -931 to -351 HU with an average value of -748 HU. This suggests an increase in the air component of the composition of the lung tissue after preservation in MTMS. The volume of the lungs changes significantly from an initial volume of 1.32 cm³ to a final volume of 2.43 cm³ as reported in Figure 4-13 and Figure 4-14. This increase in volume is likely due to the changes in HU values described previously. The maximum distance measurement was constant at 3.0 cm before and after the MTMS preservation.



Figure 4-13. Pre MTMS preservation lung CT image and analysis. Volumetric, maximum distance, and HU measurements of the lung of Ratigan before MTMS plastination were analyzed using 3-D modeling image processing.



Figure 4-14. Post MTMS preservation lung CT image and analysis. Volumetric, maximum distance, and HU measurements of the lung of Ratigan after MTMS plastination were analyzed using 3-D modeling image processing.

4.2 POLYETHYLENE GLYCOL (PEG)

As expected, the rat preserved in PEG (Splinter) was soft to the touch and pliable. The outgassing of the PEG preservation chemicals was quite strong and persisted for over two weeks. The specimen became oily and greasy after the completion of the impregnation process. The skin tone did not change noticeably from its original state. The weight change from the preservation process was a decrease from 0.535 kg to 0.411 kg.

In the weeks after the PEG impregnation process was completed, the specimen developed black spots on its abdomen and yielded a foul stench. Prior to the preservation process, the animal was externally rinsed, but the internal organs were not emptied and washed. The PEG and acetone mixture was not injected into the tissue but allowed to diffuse into the cellular matrix from an external bath, and the entire process was performed at standard pressure. Therefore it is apparent that the PEG impregnation procedure was not complete. This is noted for future studies.

4.2.1 DXA Results

The tissue composition measurements of Splinter were analyzed using DXA on the same date and time as Ratigan before and after their respective preservation procedures and are reported in Table 4-2.

Table 4-2. DXA Measurements of pre and post PEG preservation of Splinter. The tissue compartment masses for bone mineral content (BMC), fat, and lean tissues are included and calculated using the total mass and DXA measurements.

	Total Mass (kg)	BMC (g)	Fat (g)	Lean Tissue (g)
Initial	0.535	14.6	41	479
Final	0.411	13.5	51	347

The initial tissue composition percentage is 2.7 percent for bone mineral content and 3.2 percent for the final, resulting in an increase of 0.6 percent. The preservation procedure did not significantly change the mass of the bones. The lean muscle mass tissue composition percentage decreased 5.1 percent, which is a much less significant change when compared to the MTMS results. Likewise, the tissue composition change for fat tissue is 4.7 percent. This small change is likely due to the density changes arising from dehydration of the fat tissues and uptake of the PEG material and supports the hypothesis that PEG is a good tissue analog for density because of its similar chemical structure to human tissue.

4.2.2 CT Results and Analysis

Total body images and images of important organs before and after the PEG preservation procedure were taken and reported in this section. The pre-preservation scan is shown in Figure 4-15. Measurements of the change in the HU values, size, and shape of these organs from before and after the preservation were made using the CT imaging processing software. Splinter was smaller than Ratigan and less anatomic detail was able to be identified. The measurements described include volumetric analysis of the brain, kidney, and lungs and changes to the HU values for the brain, skin, bone, kidney, and lungs.

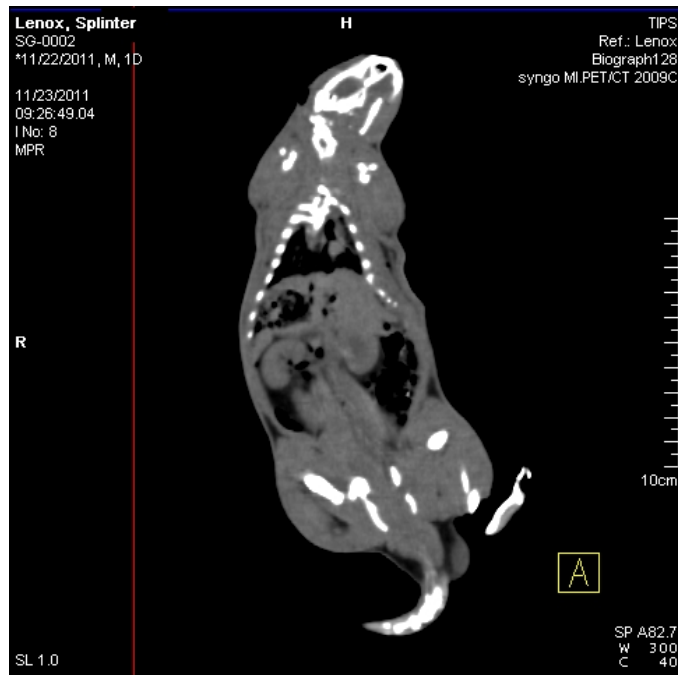


Figure 4-15. Initial total body image of Splinter before PEG impregnation.

The PEG preservation process appeared to decrease the contrast between the internal organs and homogenized the HU values of some of the tissues, and therefore more detail in organs was able to be imaged and identified before the preservation process. Air bubbles in the post PEG preservation total body image in Figure 4-16 suggest that the PEG preservation did not fully penetrate the tissues and that the tissues were undergoing decomposition.

The initial range of the brain tissue was -130 to 290 HU with an average of 86 HU. The HU measurements lowered significantly after preservation, ranging from -708 to -44 HU with an average value of -249 HU. This is likely due to the preservation chemicals not penetrating through the skull and means an increase in the air composition component of the tissue.

Volumetric analysis of the brain tissue performed on the initial scan of Splinter was 0.67 cm³ and appeared to increase to 1.09 cm³. This is likely related to the very low final HU values calculated for the brain tissue. Before and after photos are in Figure 4-17 and Figure 4-18.

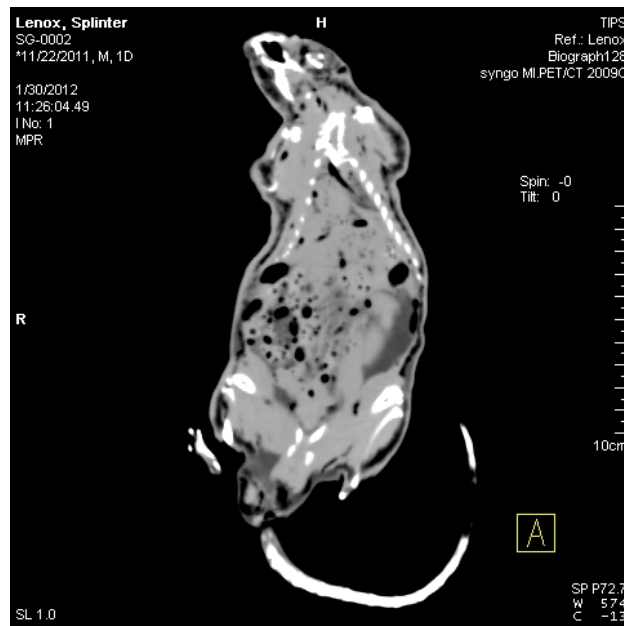


Figure 4-16. Total body image after PEG impregnation of Splinter.

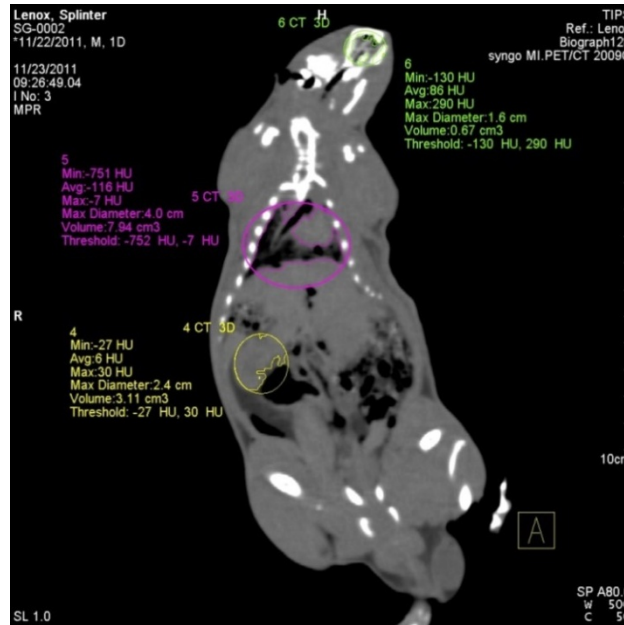


Figure 4-17. Pre PEG impregnation brain, lungs and kidney CT image and analysis. Initial HU values and volume measurements of the brain(6), lungs (5) and kidney (4) of Splinter before PEG impregnation were analyzed using 3-D modeling image processing.

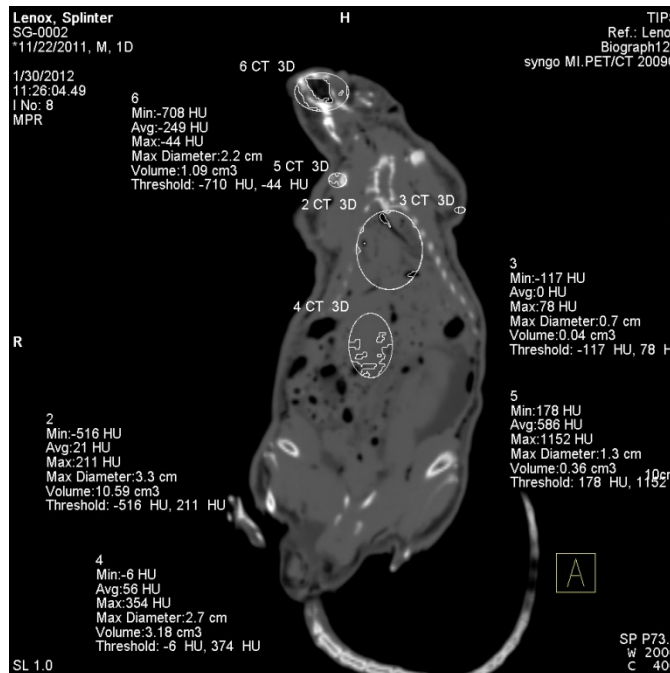


Figure 4-18. Pre PEG impregnation brain, lungs, kidney, skin, and bone CT image and analysis. Final HU values and volume measurements of the brain (6), lungs (2) and kidney (4) and HU measurements of skin (3) and bone (2) of Splinter before PEG impregnation were analyzed using 3-D modeling image processing

The initial skin HU values range from -80 to 6 HU with an average value of -45 HU and are reported in Figure 4-19. The final skin HU values range from -117 to 78 HU with an average of 0 HU. The initial bone HU measurements ranged from 220 to 1417 HU and averaged 588 HU. The final HU measurements ranged from 178 to 1152 and averaged 586 HU and are reported in Figure 4-20.



Figure 4-19. Pre PEG impregnation analysis of skin. Initial skin average and range of HU values for Splinter before PEG impregnation were measured using 3D image processing software.



Figure 4-20. Pre PEG impregnation analysis of bone. Initial bone average and range of HU values for Splinter before PEG impregnation were measured using 3D image processing software.

The lung volume in Splinter calculated before PEG preservation was 7.94 cm³ and the final volume appeared to increase to 10.59 cm³. This is likely due to the significant increase in HU values calculated for the lung tissue. Initially the HU values ranged from -751 to -7 HU with an average of -116. After preservation the average HU value was found to be 21 HU and ranged from -6 to 354 HU. The final HU values for the lungs are similar to the HU values calculated for the surrounding tissue, which is not expected. If the radiological properties were unchanged or even proportional to the original there should be a clear difference between the surrounding tissues and the lung tissue.

The HU values for the kidney ranged from -27 to 30 HU with an average of 6 HU and after PEG impregnation increased to a range of -6 to 354 HU and an average of 56. This is likely related to the PEG impregnation appearing to homogenize HU values of the soft tissues, as seen previously in the final HU values of the lung tissue. The initial volume of the kidney was 3.11cm^3 and shrank to 2.7cm^3 after the PEG plastination process, also likely related to the HU discrimination problems resulting from the addition of PEG to the tissues.

5. CONCLUSIONS AND FUTURE WORK

The uses of both DXA and CT proved to be valuable tools in assessing the viability of the preservation techniques for use in developing phantoms. Additionally, the selection of MTMS and PEG provided an insightful assessment of two very different preservatives.

The initial scanning of each of the rats using DXA and CT was successful and provided a standard for results to compare the specimens after preservation. Ratigan was larger and provided better CT imaging both before and after preservation when compared to Splinter and the PEG preservation. However, MTMS preservation still affected the HU values and many internal organs such as the liver and brain shrank after the completion of the plastination process. The PEG preservation appeared to have air pockets and homogenized HU numbers in the final CT scans of the specimen.

The PEG preservation had much more accurate tissue composition measurements when compared to the original tissue composition values that were calculated by DXA. The BMC was fairly accurate and unchanged for both MTMS and PEG preservation procedures, but DXA greatly overestimated the lean tissue measurements after MTMS preservation and calculated them to be much greater than the total mass. The DXA also greatly underestimated the fat content, calculating an impossible negative mass.

The MTMS process outlasted the PEG preservation procedure. The PEG preservation likely did not penetrate the tissues and continued to decompose in the

weeks following the experiment. Ratigan, after the completion of the MTMS preservation, is still preserved 3 years later.

In future study, the specimen should be injected with the PEG solution to allow better access to the internal organs and tissues and the dehydration and bulking procedures should be performed under a vacuum to determine if this improves the success of the PEG impregnation for a whole body organism. Improving uptake of the PEG into the tissues would also validate the contribution of the PEG preservation to the change in HU values for the organs seen in this investigation. Increasing the size of the specimen may also improve CT imaging ability.

For future investigations of the MTMS preservation processes, two approaches should be considered: initial dehydration of the tissue in acetone to promote bulking of the MTMS into the tissue or the injection of MTMS into the specimen instead of relying on diffusion as the primary means of penetration. Direct injections would also determine whether subdermal accumulation of MTMS is a result of diffusion and may better preserve the tissues that are protected by skeletal structures like the brain.

Further study of the imaging quality provided by these preservation techniques to analyze differences in the structure and anatomy of the specimens may be better demonstrated using a Micro-CT scanner. Micro-CT provides much finer resolution than the CT scanner used in this investigation and would be useful in capturing increasingly detailed anatomical images of small animals and monitoring the progression of changes.

REFERENCES

- Berger MJ, Hubbell JH. X-Ray and Gamma-Ray Data [online]. Available at: http://www.nist.gov/pml/data/xray_gammaray.cfm. Accessed May 12, 2013.
- Casazza JP, Felver ME, Veech RL. The Metabolism of Acetone in Rat. *Journal of Biological Chemistry* 259: 231-236; 1984.
- CDC. Center for Disease Control. Overweight and Obesity [online]. Available at: <http://www.cdc.gov/obesity/index.html>. Accessed 04 May 2014.
- GEHealthcare. Lunar Prodigy DXA User Manual. 2012.
- Genton L, Hans D, Kyle U, Pichard C. Dual-energy X-ray absorptiometry and body composition: differences between devices and comparison with reference methods. *Nutrition* 18: 66-70; 2002.
- Greene EC. *Anatomy of the Rat*. Philadelphia: The American Philosophical Society; 1935.
- Hagens G. The Current Potential of Plastination. *Anatomy and Embryology* 175: 441-421; 1987.
- Hagens Gv. Heidelberg Plastination Folder: Collection of Technical Leaflets of Plastination. 2 ed. Heidelberg, Germany: Biodur Products; 1986.
- Harp JB. Obesity in the National Football League. *Journal of the American Medical Association* 293: 1061-1062; 2005.
- Hasenfuss G. Animal models of human cardiovascular disease, heart failure and hypertrophy. *Cardiovascular Research* 39: 60-76; 1998.
- Herman GT. *Fundamentals of Computerized Tomography: Image Reconstruction from Projections*. Springer Publishing Company, Incorporated; 2009.
- ICRU. ICRU Report No. 44: Tissue substitutes in radiation dosimetry and measurement. Bethesda, MD: International Commission on Radiation Units & Measurements, Inc; 1989.
- Jackson AS, Pollock ML. Generalized equations for predicting body density of men. *British Journal of Nutrition* 40: 497-504; 1978.

- Jackson AS, Pollock ML, Ward A. Generalized equations for predicting body density of women. *Medicine and Science in Sports and Exercise* 12: 175-182; 1980.
- Jackson AS, Stanforth PR, Gagnon J, Rankinen T, Leon AS, Rao DC, Skinner JS, Bouchard C, Wilmore JH. The effect of sex, age and race on estimating percentage body fat from body mass index: The Heritage Family Study. *International Journal of Obesity and Related Metabolic Disorders* 26: 789-796.; 2002.
- Kohrt WM. Body Composition by DXA: Tried and True? *Medicine and Science in Sports and Exercise* 27: 1349-1353; 1995.
- König HE, Probst A, Dier H, Sora MC. Production of Anatomical Specimens for Teaching Practice in Veterinary Anatomy by Means of Polyethylene Glycol (PEG) Impregnation. A Comparison with the Method of Plastination. *Chilean Journal of Agricultural and Animal Sciences, ex Agro-Ciencia* 29: 59-64; 2013.
- Lelovas PP, Xanthos TT, Thoma SE, Lyritis GP, Dontas IA. The Laboratory Rat as an Animal Model for Osteoporosis Research. *Comparative Medicine* 58: 424-430; 2008.
- Lochmüller E, Jung V, Weusten A, Wehr U, Wolf E, Eckstein F. Precision of high-resolution dual energy X-ray absorptiometry of bone mineral status and body composition in small animal models. *European Cells and Materials* 1; 2001.
- Olds RJ, Olds JR. *The Color Atlas of The Rat - Dissection Guide*. New York, New York: John Wiley & Sons; 1979.
- Pietrobelli A, Heymsfield SB, Wang ZM, Gallagher D. Multi-component body composition models: recent advances and future directions. *European Journal of Clinical Nutrition* 55: 69-75; 2001.
- Rose BS, Flatt WP, Martin RJ, Lewis RD. Whole Body Composition of Rats Determined by Dual Energy X-Ray Absorptiometry Is Correlated with Chemical Analysis¹. *The Journal of Nutrition* 128: 246-250; 1998.
- ScienceLab.com. Polyethylene Glycol [Material Safety Data Sheet]. 2005.
- Seco J, Evans PM. Assessing the effect of electron density in photon dose calculations. *Medical Physics* 33: 540-552; 2006.
- Serendip. Comparing Brain and Body Size [online]. Available at: <http://serendip.brynmawr.edu/bb/kinser/Int3.html>. Accessed May 1, 2014.
- Sigma-Aldrich. Trimethoxymethylsilane [Material Safety Data Sheet]. 2012.

- Silverthorn DU. *Human Physiology: An Integrated Approach*. 4th ed. San Francisco: Pearson Education, Inc.; 2007.
- Siri WE. *Body Composition from Fluid Spaces and Density: Analysis of Methods*. Berkeley, California: Lawrence Radiation Laboratory; 1956.
- Slosman D, Casez J, Pichard C, Rochat T, Fery F, Rizzoli R, Bonjour J, Morabia A, Donath A. Assessment of whole-body composition with dual-energy x-ray absorptiometry. *Radiology* 185: 593-598; 1992.
- Smith CW. *Conservation of Waterlogged Leather Using Polymers*. Report 4. College Station, Texas: Archaeological Preservation Research Laboratory; 1997.
- Smith CW. *Re-treatment of a PEG Treated Composite Artifact - A Sabot*. Report 3. College Station, Texas: Archaeological Preservation Research Laboratory; 1997.
- Smith CW. *Re-treatment of PEG Treated Waterlogged Wood*. Report 2. College Station, Texas: Archaeological Preservation Research Laboratory; 1997.
- Smith CW. *Silicone and Polymer Technologies*. Report 1. College Station, Texas: Archaeological Preservation Research Laboratory; 1997.
- Smith CW. *Conservation of Waterlogged Corncobs Using Silicone Oils*. Report 8. College Station, Texas: Archaeological Preservation Research Laboratory; 1998.
- Smith CW. *Polymerization of PR-10, PR-12 and PR-14 Silicone Oils in Animal Hides Using Catalyst Fumes - Keratin and Amino Acids Cross Linking*. Report 12. College Station: Archaeological Preservation Research Laboratory; Report 12; Report 12; 1998.
- Smith CW. *Polymerization of PR-10, PR-12 and PR-14 Silicone Oils in Animal Hides Using Catalyst Fumes - Keratin and Amino Acids Cross Linking*. Report 18. College Station: Archaeological Preservation Research Laboratory; Report 18; Report 18; 1998.
- Smith CW. *Silicone Oil: A New Technique for Preserving Waterlogged Rope*. Report 5. College Station, Texas: Archaeological Preservation Research Laboratory; 1998.
- Smith CW, Hamilton DL. *Comparison of the Bulking Abilities of Polyethylene Glycol 1450 and PS341 Silicone Monomers*. Report 20. College Station, Texas: Archaeological Preservation Research Laboratory; 1998.
- Smith CW, Hamilton DL. *Conservation of 17th Century Canvas Using Silicone Oils*. Report 6. College Station, Texas: Archaeological Preservation Research Laboratory; 1998.

- Smith CW, Hamilton DL. Conservation of Devitrified Glass with Methylhydrocyclosiloxanes and Silicone Oils. Report 15. College Station, Texas: Archaeological Preservation Research Laboratory; 1998.
- Smith CW, Hamilton DL. Conservation Research Laboratory (CRL) Leather Dressing. Report 10. College Station, Texas: Archaeological Preservation Research Laboratory; 1998.
- Smith CW, Hamilton DL. Consolidation of Formalin Treated Marine Crustacean Specimens Using Silicone Oils. Report 9. College Station, Texas: Archaeological Preservation Research Laboratory; 1998.
- Smith CW, Hamilton DL. Induced Flash Polymerization using Low Neutron Flux Radiation. Report 22. College Station, Texas: Archaeological Preservation Research Laboratory; 1998.
- Smith CW, Hamilton DL. Mass Spectrographic Analysis of Out Gasses Created from the Dehydration of Archaeological Wood Samples. Report 11. College Station, Texas: Archaeological Preservation Research Laboratory; 1998.
- Smith CW, Hamilton DL. Polymerization of Archaeological Waterlogged Wood Treated with Polyethylene Glycol. Report 19. College Station, Texas: Archaeological Preservation Research Laboratory; 1998.
- Smith CW, Hamilton DL. Polymerization of Polyethylene Glycol and Glycerine. Report 16. College Station, Texas: Archaeological Preservation Research Laboratory; 1998.
- Smith CW, Hamilton DL. Polymerization Potentials of Polyethylene Glycol Compounds Commonly Used in Archaeological Artifact Conservation. Report 17. College Station, Texas: Archaeological Preservation Research Laboratory; 1998.
- Smith CW, Hamilton DL. Preservation of a Dog Heart Using Silicone Oils. Report 12. College Station, Texas: Archaeological Preservation Research Laboratory; 1998.
- Smith CW, Hamilton DL. Preservation of a Dog Heart Using Silicone Oils: A Second Approach. Report 13. College Station, Texas: Archaeological Preservation Research Laboratory; 1998.
- Smith CW, Hamilton DL. Preservation of Kelp Specimens. Report 14. College Station, Texas: Archaeological Preservation Research Laboratory; 1998.
- Smith CW, Hamilton DL. Silicone Bulking of Waterlogged Cork Using PS340, PS341 and PS343. Report 7. College Station, Texas: Archaeological Preservation Research Laboratory; 1998.

- Smith CW, Hamilton DL. Tanning of Animal Hides Using Silicone Oils. Report 21. College Station, Texas: Archaeological Preservation Research Laboratory; 1998.
- Smith CW, Hamilton DL. Treatment of Waterlogged Wood Using Hydrolyzable, Multi-Functional Alkoxysilane Polymers. Report 23. College Station, Texas: Archaeological Preservation Research Laboratory; 1998.
- Starks EC, Cutter RD. The Dissection of the Rat. 3 ed. Stanford University, California: Stanford University Press; 1931.
- Tothill P, Laskey M, Orphanidou C, Wijk Mv. Anomalies in dual energy X-ray absorptiometry measurements of total-body mineral during weight change using Lunar, Hologic, and Norland instruments. *British Journal of Radiology* 72: 661-669; 1999.